A Comparative Kinetic and Thermodynamic Perspective of the σ-Competition Model in *Escherichia coli*

Abantika Ganguly and Dipankar Chatterji*
Molecular Biophysics Unit, Indian Institute of Science, Bangalore, India

ABSTRACT Transcription is the most fundamental step in gene expression in any living organism. Various environmental cues help in the maturation of core RNA polymerase (RNAP; $\alpha_2\beta\beta'\omega$) with different σ-factors, leading to the directed recruitment of RNAP to different promoter DNA sequences. Thus it is essential to determine the σ-factors that affect the preferential partitioning of core RNAP among various σ-actors, and the role of σ-switching in transcriptional gene regulation. Further, the macromolecular assembly of holo RNAP takes place in an extremely crowded environment within a cell, and thus far the kinetics and thermodynamics of this molecular recognition process have not been well addressed. In this study we used a site-directed bioaffinity immobilization method to evaluate the relative binding affinities of three different *Escherichia coli* σ-factors to the same core RNAP with variations in temperature and ionic strength while emulating the crowded cellular milieu. Our data indicate that the interaction of core RNAP-σ is susceptible to changes in external stimuli such as osmolytic and thermal stress, and the degree of susceptibility varies among different σ-factors. This allows for a reversible σ-switching from housekeeping factors to alternate σ-factors when the organism senses a change in its physiological conditions.

INTRODUCTION

Initiation of transcription is the most fundamental step in controlling the gene expression of prokaryotes. Although there are a multitude of interaction interfaces between DNA and RNA polymerase (RNAP), the focal point of interest is the contact of RNAP with a promoter (1,2). For example, *Escherichia coli* possesses seven different σ-factors (σ^{70}, σ^{38}, σ^{32}, σ^{F}, σ^{E}, σ^{fecI}, and σ^{54}), each of which has its own unique promoter sequence that acts as a genetic switch for the positive regulation of transcription (3,4). Therefore, global regulation of transcription is determined by the competition among different σ-factors to bind to the same core RNAP (5,6). Earlier studies indicated that fluctuations in the cellular levels of different σ-factors alone are not responsible for the altered gene product pattern observed in bacteria (7). It follows, then, that preferential partitioning of core RNAP among σ-factors must depend on the relative binding affinities of the σ-factors under changing physiological conditions. Several estimates of core RNAP-σ interactions are available in the literature (8–11); however, they were obtained under different experimental conditions. As such, a direct comparison among them is not possible and we cannot predict the role of the σ-competition model in global gene regulation. These previous studies also did not explore the effect of temperature, although thermal stress is one of the important external stimuli responsible for changing the transcription pathway from the housekeeping σ-factor to the alternative σ-factors. Further, the macromolecular assembly of holo RNAP takes place in an extremely crowded environment within a cell, and thus far the kinetics and thermodynamics of this molecular recognition process have not been well addressed.

Recent research showed that macromolecular crowding can exert significant effects on the kinetic pathways of reactions (12). Thus, methodological and conceptual advances are necessary to take into consideration these nonideality effects. In this work, we performed a systematic and quantitative comparison of the binding affinities of housekeeping σ-factor in *E. coli* (σ^{70}) (13) and two other stress-related σ-factors (σ^{38} and σ^{32}) (14,15) under changing conditions of osmolarity and temperature. We used site-directed and bioaffinity-based immobilization methods to interrogate the core RNAP-σ interaction under conditions of macromolecular crowding to obtain a more practical understanding of σ-switching in vivo. By making use of the Langmuir-Blodgett (LB) method and surface plasmon resonance (SPR), we were able to analyze the interactions for real-time kinetics as well as equilibrium-binding thermodynamics. Our data indicate that although the interaction of core RNAP-σ^{70} is strongest under physiological conditions, it is extremely susceptible to changing external stimuli and hence allows for a reversible σ-switching to alternative σ-factors under conditions of osmolytic and thermal stress.

MATERIALS AND METHODS

Purification of recombinant *E. coli* RNAP subunits

C-terminally His-tagged α-subunit (α-His) (16) was purified under native conditions by Ni-NTA affinity chromatography. The core subunits β, β', and ω did not have any tag and were purified from inclusion bodies according to a standardized protocol (17). All three σ-factors were untagged and were purified from inclusion bodies as described by Tanaka et al. (14) from strain pARC81112 (σ^{70}) and plasmids pET3b and pET21H overexpressing σ^{38} and σ^{32}, respectively. We estimated the σ-protein concentration using

Submitted April 2, 2012, and accepted for publication August 2, 2012.

*Correspondence: dipankar@mbu.iisc.ernet.in

Editor: Kathleen Hall.

0006-3495/12/09/1325/9 $2.00

http://dx.doi.org/10.1016/j.bpj.2012.08.013

the Bradford assay at 3 mg/ml, 2 mg/ml, and 2 mg/ml for σ^{70}, σ^{38}, and σ^{32}, respectively (Fig. 1).

In vitro reconstitution of *E. coli* RNAP from recombinant subunits

In vitro reconstitution of core RNAP was carried out according to the protocol described in Tang et al. (18) with slight modifications. The reconstituted mixture was first passed through a Ni-NTA column matrix (see Fig. S1 *a* in the Supporting Material) and then further clarified by passage through a Heparin-Sepharose column equilibrated with TGED (10 mM Tris-HCL, pH 7.9 at 4°C; 0.1 mM EDTA; 0.1 mM DTT; 5% glycerol) with 150 mM NaCl to eliminate any excess His-tagged α that might have eluted from Ni-NTA column. The protein was eluted with TGED with 600 mM NaCl. The fractions were checked for the presence of core RNAP on a 10% SDS-PAGE gel (Fig. S1 *b*). Fractions containing reconstituted core RNAP were pooled together and concentrated by ultracentrifugation. The protein concentration was estimated via a Bradford assay at 2.6 mg/ml. Data related to the details of protein purification, reconstitution of core RNAP, and generation of Scatchard plots and van 't Hoff plots used for the kinetic and thermodynamic analyses are provided in the Supporting Material.

Formation of the NiA-HisRNAP/NiA-HisRNAP-σ LB monolayer

The Ni-arachidate monolayer was formed on an LB trough (Nima Technology, Coventry, UK) by spreading 25 μl of 1 mg/ml arachidic acid dissolved in chloroform (HPLC grade; Merck, Rahway, NJ) on 200 ml of $NiSO_4$ solution (pH 7.4 with 2 mM Tris-HCL buffer and 10 mM NaCl) at a concentration of 10^{-4}M (Milli-Q water, resistivity 18.2 MΩ. cm). At this pH, the carboxyl group of arachidate molecules will remain ionized and interact with the Ni^{+2} present in the subphase to form a Ni-arachidate template (19). To form the NiA-HisRNAP monolayer, core HisRNAP was injected just below the preformed NiA monolayer after 30 min to a final concentration of 7.4 nM. To study the interaction of the σ-subunit with core HisRNAP, we injected different amounts of σ-subunit (3.7–23 nM) below the preformed NiA-HisRNAP monolayer after ensuring that NiA-HisRNAP monolayer had reached equilibrium (over a period of 6 h). There was no stirring of the subphase after the injection of proteins, and the barrier speed for performing all of the pressure-area (P-A) isotherm measurements was 20 cm^2/min. The area/molecule values for kinetic experiments were estimated at a surface pressure of 12 mN/m when the monolayer was in its condensed state. To evaluate the area/molecule changes due to addition of σ-subunit, we recorded P-A isotherms 1 h after injecting the σ-subunit. The temperature of the trough was maintained at $T \pm 0.1$°C with the help of a thermostat bath attached to the trough. The trough was placed under a Perspex box to avoid any dust.

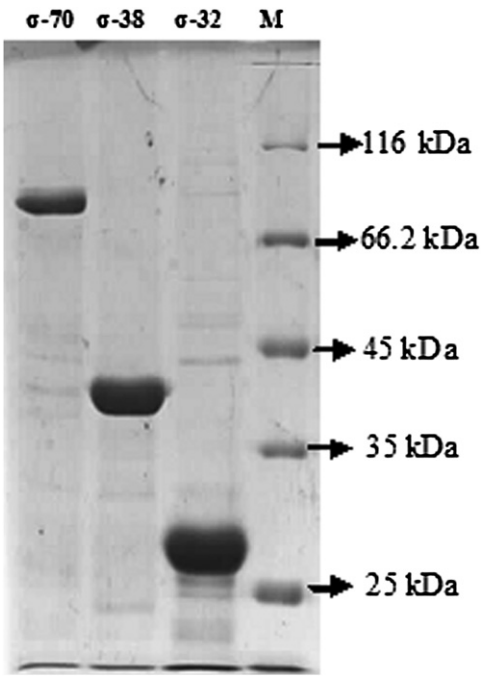

FIGURE 1 Purification profile of σ^{70}, σ^{38}, and σ^{32} on a 10% SDS-PAGE. The migration position of the marker is shown on the right.

SPR studies

The binding experiments were carried out in a BIAcore 3000 using a CM5 chip. The σ-factors were diluted to a concentration of ~400–600 pM in 10 mM sodium acetate buffer, pH 4.0, and injected over the activated flow cells at a flow rate of 2 μl/min until a response unit (RU) change of 1000–1200 RU was obtained. Channel 1 was left underivatized to correct for nonspecific binding. To follow the kinetic interactions, we allowed 50 μl of core RNAP at the desired concentration (200–600 mM) in HEPES-buffered saline running buffer (10 mM HEPES, pH 7.4, 150 mM NaCl, 3 mM EDTA, and 0.005% Polysorbate-20) to flow over all of the channels at 10 μL/min. The chip was regenerated with 10–20 μl of 10 mM NaOH at a flow rate of 50 μL/min, followed by washing with the running buffer until the baseline stabilized.

RESULTS

Probing the protein-protein interaction at the air-water interface

We evaluated the binding of core RNAP to different σ-factors using the LB technique. This technique detects macromolecular interactions by observing changes in instantaneous surface tension ($\gamma_0 - \gamma$) as a result of molecular interactions at the interface (20,21). Although the LB technique is frequently used for quantitative evaluations of surface-active molecules such as polymers and phospholipids (22), its use to follow the activity of nonsurface-active biomacromolecules has been restricted. Recently, our laboratory used the unique property of fatty acids to spread as isotropic lamellar structures on aqueous solutions, as well as their ability to interact with divalent cations (Ni^{+2}), to successfully modify the LB technique. We demonstrated the ability of Ni(II)-ion coordinated arachidic acid (NiA) monolayers to provide a two-dimensional scaffold for characterizing and quantitatively assaying sequence-specific RNAP-T7A1 promoter DNA interactions under conditions of molecular crowding (19). His-tagged core RNAP was regioselectively immobilized at the air-water interface (as described in Materials and Methods). This ensured that despite its immobilization, the polymerase retained sufficient mobility for the σ-interaction interfaces (located mainly on the β and β' subunits) to remain exposed. Site-directed immobilization ensured a homogeneous surface density of molecules, and the specificity of the coordination

bond (180–200 kcal/mol) both minimized nonspecific adsorption and allowed us to probe noncovalent protein-ligand interactions (0.6–2.59 kcal/mol) without any surface leaching of the bound molecules (16). The restriction in the degrees of freedom of the molecules took care of protein aggregation and other side reactions without affecting the intrinsic binding interfaces between the cognate partners. However, in contrast to conventional bioaffinity immobilization techniques, immobilization at the air-water interface allowed us to study the reactions in a physiologically compatible buffer system without any loss of functional activity of the biomolecule.

Nonobligatory heterocomplexes such as RNAP ($\alpha_2\beta\beta'\omega\sigma$), which are assembled dynamically in response to cellular needs, are very susceptible to changes in osmolarity. Hence, it is essential to define the ionic strength of the medium in which the free energy of the complex is optimized. In a previous work (23), we showed that increasing concentrations of monovalent Na^+, beyond a concentration range of 0–25 mM NaCl, compromised the rigidity of the monolayer by lowering the condensation effect of a divalent ion like Ni^{+2}. For RNAP-σ interactions, optimized binding was observed at a salt concentration of 10 mM NaCl. Although this ionic strength is low compared with the physiological ionic strength usually maintained for in vitro studies (0.05–0.15 M NaCl or KCl) (24), we should keep in mind that the requirement of ionic strength to study macromolecular interactions at the interface is different.

σ-Competition model evaluated using the LB technique

To compare the binding affinities of different σ-factors for core RNAP, we first evaluated the kinetic parameters of the core RNAP- σ^{70} interaction by conducting a saturation binding experiment at 25°C (25). Fig. 2 *a* (*inset*) shows the immobilization of 7.4 nM of core HisRNAP at the NiA monolayer. The P-A isotherms were checked for hysteresis over a period of 6 h until the area/molecule value for NiA-HisRNAP reached equilibrium. This ensured that the changes we observed after injecting the different σ-factors were due to the core-σ interaction alone, and ruled out any contribution from excess His-RNAP present at the monolayer. After ensuring that NiA-HisRNAP monolayer had reached equilibrium, we injected σ^{70} at the monolayer in increasing amounts until saturation was reached, as indicated by no further increase in area/molecule values upon addition of σ-subunit. Fig. 2 *a* shows the P-A isotherms for the NiA–HisRNAP-σ^{70} monolayer when different mole fractions of σ^{70} were injected relative to a fixed concentration of His-RNAP at 25°C. Saturation was reached for a core/σ molar ratio of 1:3. In all cases, the initial concentration of the ligand was kept to at least 10 times the probable K_D value to achieve 90% occupancy. Assuming that because HisRNAP is bound directly at the monolayer, it is responsible for showing surface activity, and σ^{70} does not have any distinct surface activity, we generated a fractional saturation plot (ν versus L) for the binding of different fractions of σ^{70} to a fixed amount of core His-RNAP (25). The fractional saturation (ν) of His-RNAP with σ^{70} was determined using the equation

$$\nu = \frac{A_t - A_o}{A_{max} - A_o}, \tag{1}$$

where A_t is the area per molecule value of the NiA–HisRNAP-σ^{70} monolayer at any intermediate concentration of σ^{70}, A_o is the area per molecule of only NiA-HisRNAP, and A_{max} is the area per molecule of NiA-HisRNAP-σ^{70} at saturation. Assuming that the reaction has been allowed to proceed to equilibrium, a fractional saturation plot is then generated for the saturation binding of the ligand to the analyte. For a simple equilibrium reaction,

$$K_D = \frac{[AL]}{[A][L]}. \tag{2}$$

Again,

$$\nu = \frac{[AL]}{[A] + [AL]}, \tag{3}$$

where K_D is the apparent dissociation constant, *[AL]* is the concentration of core RNAP bound to σ, *[A]* is the unbound core RNAP (analyte), and *[L]* is the unbound σ (ligand) given by

$$L = L_0 - \nu A_0, \tag{4}$$

where A_0 and L_0 are the total core RNAP and σ-concentration, respectively.

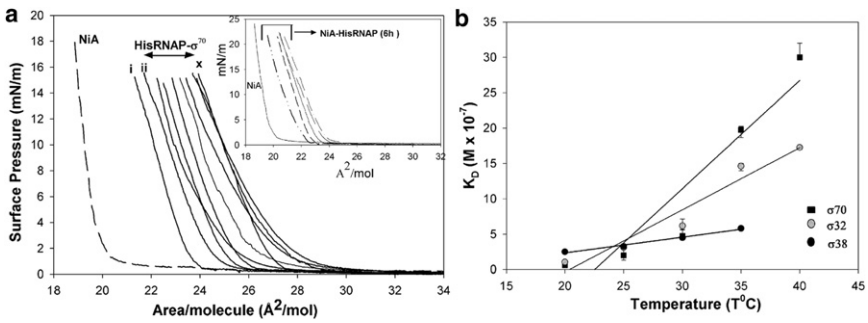

FIGURE 2 (*a*) From left to right, P-A isotherms of NiA and NiA-HisRNAP with different amounts of σ^{70} in a molar ratio of (i) 1:0, (ii) 1:0.75, (iii) 1:1, (iv) 1:1.2, (v) 1:1.3, (vi) 1:1.5, (vii) 1:1.75, (viii) 1:2.1, (ix) 1:2.5, and (x) 1:3.1 at 20 mM NaCl until saturation was achieved. (*Inset*) From left to right, P-A isotherms of NiA and NiA-HisRNAP (7.4 nM) over a period of 6 h at 25°C and 10 mM NaCl, until equilibrium was reached. (*b*) Plot showing the variation of macroscopic dissociation constant values with change in temperature for the binding of core RNAP with σ^{70}, σ^{32}, and σ^{38}.

Combining Eqs. 2 and 3 gives

$$\nu = \frac{[L]}{K_D + [L]}. \quad (5)$$

The nonlinear rectangular hyperbola fit was linearized for easier analysis (Fig. S2 *a*) using the Scatchard equation:

$$\frac{\nu}{L} = \frac{1}{K_D} - \frac{\nu}{K_D}. \quad (6)$$

From the slope, the dissociation equilibrium constant was determined as $K_D = 5.00\ (\pm 0.66) \times 10^{-9}$ M, and the number of binding sites (n) was one. From the equilibrium constant, the Gibbs free energy of reaction (ΔG_r) was calculated as

$$\Delta G_r = -RT \ln K_A = RT \ln K_D = 2 \times 298 \times (-19.114)\ \text{kcalmol}^{-1}, \quad (7)$$

where R is the gas constant and T is the absolute temperature. This gave a value of $\Delta G_r = -11.39\ (\pm 1.2)$ kcal mol^{-1} of the free energy of reaction at 25°C for the overall process.

A similar kinetic analysis was carried out for the binding of His-RNAP with σ^{32} and σ^{38} at the interface under the same experimental conditions (Fig. S2, *b* and *c*). The binding affinities for each σ-factor with core RNAP at 25°C and in the presence of 10 mM NaCl, along with their respective free energies of interaction are given in Table 1. From the values, it is evident that at 25°C and in the presence of 20 mM NaCl, the relative binding affinity of core RNAP with different σ-factor varies as σ-38 < σ-32 << σ-70.

Temperature sensitivity of core RNAP-σ binding at the LB monolayer

The binding of σ^{70}, σ^{32}, and σ^{38} with core RNAP was estimated over a temperature range of 20–40°C. We followed the interaction beyond the physiological temperature because heat-shock gene products are known to come into play at temperatures of ≥42°C. Thus, we wanted to study the affinity of stress-related σ-factors (σ^{H} and σ^{S}) at the temperature at which their functional role is optimized. However, one should keep in mind that these were in vitro studies carried out with pure components, and the effect of other cellular components could not be traced. The variation in macroscopic dissociation constant values with temperature is tabulated in Table 2. From the presented data, it is evident that the binding affinity of all three σ-factors decreases with an increase in temperature. However, the temperature sensitivity of this interaction varies as σ-38 < σ-32 < σ-70.

Fig. 3 gives a qualitative indication of temperature susceptibility for the core RNAP-σ interaction. The fractional saturation plot for σ^{70} (Fig. 3 *a*) showed that at lower temperatures of 20°C, the binding was initially weak but improved with increasing concentrations of σ^{70}. The interaction showed a more uniform binding pattern at higher temperatures. Hence, the fluctuation in the estimated macroscopic dissociation constant values, and the enthalpy of formation calculated from it, is higher at the lower temperature of 20°C (11%) than at 30°C (8%). In the case of σ^{32} and σ^{38} (Fig. 3, *b* and *c*), we observed a uniform binding pattern over all of the temperature ranges, with variations in the range of 5–10%. Core RNAP binding to σ^{38} appeared to be unaffected by changes in temperature. As such, we observe a reversal in the order of relative binding affinities between σ and core RNAP as the temperature increases from 20°C to 40°C, with the crossover taking place at ~25°C (Fig. 2 *b*). Thus, at 20°C the affinity order appears to be σ-38 < σ-32 < σ-70 (in 10 mM NaCl), but at 40°C the affinity order changes to σ-70 < σ-32 < σ-38 (in 10 mM NaCl).

This reversal in the estimated affinity order is expected. Because σ^{70} is the principal σ-factor responsible for turning on genes involved with the growth of an organism, we expect it to show the strongest binding to core RNAP at optimal temperatures. However, as the organism is subjected to stress (i.e., heat shock), the binding of σ^{70} weakens to allow other σ-factors to come into play. This probably explains the greater temperature sensitivity of σ^{H} (σ^{32}) as compared with σ^{S} (σ^{38}) (Fig. 3, *b* and *c*), because the former is directly responsible for transcribing the heat-shock proteins that can buffer the organism against elevated thermal energy levels (26). The results justify our hypothesis that temperature plays a major role in controlling the transcription pathway for stress-related gene products.

We also constructed a van 't Hoff plot for the temperature range of 20–40°C (Fig. S3) for the core RNAP-σ interaction using the equation

$$\ln K_D = \frac{\Delta H}{RT} - \frac{\Delta S}{R}. \quad (8)$$

TABLE 1 Macroscopic equilibrium dissociation constant and thermodynamic constants calculated for the interaction of core RNAP with different σ-factors at 25°C and 10 mM NaCl

σ-Factor	Macroscopic dissociation constant (K_D) at 25°C (M)	Free energy of interaction (ΔG_r) at 25°C (kcal/mol)	Enthalpy of interaction (ΔH) (kcal/mol)	Entropy of interaction (ΔS) (cal/mol/K)
σ-70	$5.00\ (\pm\ 0.66) \times 10^{-9}$	−11.39 (±1.2)	−25.70 (± 4.369)	−40.00 (±8)
σ-32	$5.71\ (\pm 0.28) \times 10^{-8}$	−9.90 (±0.87)	−18.70 (± 2.8)	−22.23 (±4.01)
σ-38	$6.12\ (\pm 0.49) \times 10^{-8}$	−9.28 (± 1.02)	−9.90 (±1.02)	−1.84 (±0.22)

TABLE 2 Variation in macroscopic equilibrium dissociation constant values with temperature for core RNAP-σ interaction

Temperature	σ-70 K_D (M)	σ-32 K_D (M)	σ-38 K_D (M)
20°C	1.25 (±0.22) × 10^{-9}	2.25 (±0.11) × 10^{-8}	5.90 (±0.39) × 10^{-8}
25°C	5.00 (±0.66) × 10^{-9}	5.71 (±0.28) × 10^{-8}	6.12 (±0.49) × 10^{-8}
30°C	9.09 (±0.71) × 10^{-9}	7.29 (±0.34) × 10^{-8}	6.25 (±0.56) × 10^{-8}
35°C	1.27 (±0.10) × 10^{-8}	9.29 (± 0.31) × 10^{-8}	6.57 (±0.46) × 10^{-8}
40°C	1.58 (±0.17) × 10^{-8}	1.25 (±0.08) × 10^{-7}	-

The slope of lnK_D versus $1/T$ provides $\Delta H/R$, from which the enthalpy was calculated, and the y-intercept $\Delta S/R$ gave the entropy change of the system. The enthalpy and entropy values thus obtained are compared in Table 1. Although a negative free energy of interaction indicates that the reaction is spontaneous, the negative entropy of reaction [$\Delta S = -40.00$ (±8) cal/mol/K] coupled with a comparatively small magnitude of enthalpy [$\Delta H = -9.90$ (±1.02) kcal/mol] released indicates that the interaction may involve large-scale protein conformational changes. This is further elaborated in the Discussion section.

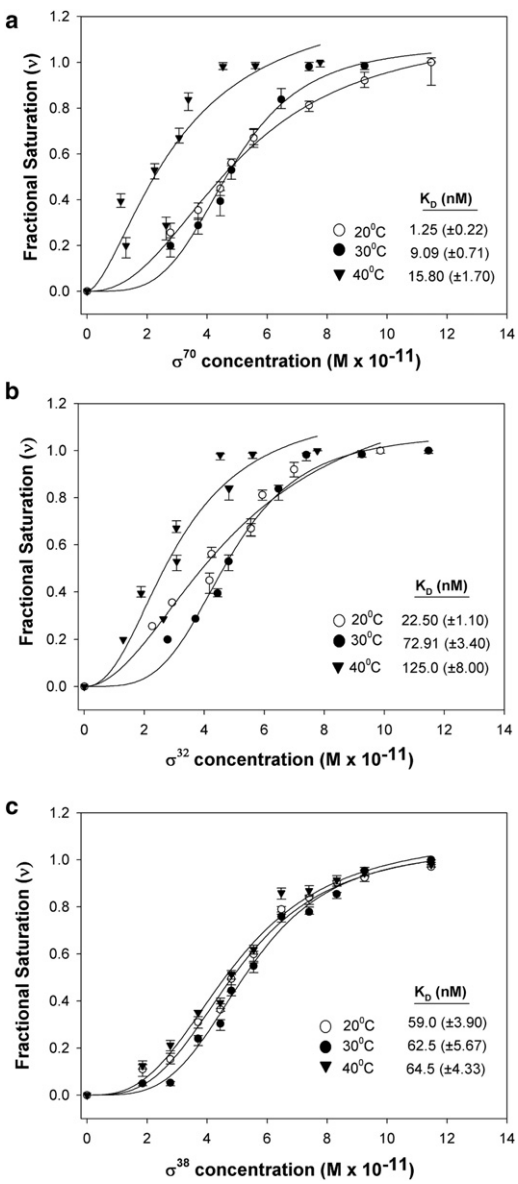

FIGURE 3 Fractional saturation plot for interaction of core RNAP with (*a*) σ^{70}, (*b*) σ^{32}, and (*c*) σ^{38} at temperatures of 20°C, 30°C, and 40°C.

Kinetic and thermodynamic evaluations of core RNAP-σ association using the SPR method

We undertook a comparative kinetic analysis for the binding of σ-factors to core RNAP by evaluating the same interactions using a different nonhomogeneous technique, SPR (Fig. S4). Here, we fitted the data globally using a nonlinear regression to determine the kinetic parameters. The concentration of σ-factors was varied between 200–750 nM for the association phase and was kept at zero during the dissociation phase. The data were fitted to a simple 1:1 Langmuir binding model ($\chi^2 = 0.73$–3.4). The kinetic parameters obtained are tabulated in Table S1. When the temperature of the system was kept invariant, the relative binding affinities of the σ-factors and kinetic parameters of core RNAP-σ binding were found to follow the same trend as observed with the LB technique.

We estimated the effect of temperature on the binding of core RNAP with σ-factor using the binding of 400 nM core RNAP with the immobilized σ-factors, within the temperature range of 20–40°C (Fig. S5 and Table S1). The values for strength of binding among the three different σ-factors, when all other variables remain unchanged, as well as the variation in binding observed with changes in temperature, correlate well with those obtained from the LB studies presented here.

Effect of ionic strength on the kinetics of the core RNAP-σ interaction

With the LB technique, we were unable to study the effect of core RNAP binding to σ-factors with variation in osmolarity of the medium. We overcame this limitation by carrying out SPR studies at ionic strengths closer to the cellular permissible limits. Fig. 4 *a* shows the sensorgrams for 400 nM of core RNAP interacting with σ^{70} in the presence of 100 mM and 150 mM NaCl at 20°C. Fig. 4 *b* shows the same interaction when it was followed at an elevated temperature of 30°C. Quantitatively, core RNAP-σ^{70} kinetics showed a pronounced salt effect at lower temperatures. Similarly, Fig. 4, *c* and *d*, show the sensorgrams for binding of the same concentration of core RNAP-σ^{32} in

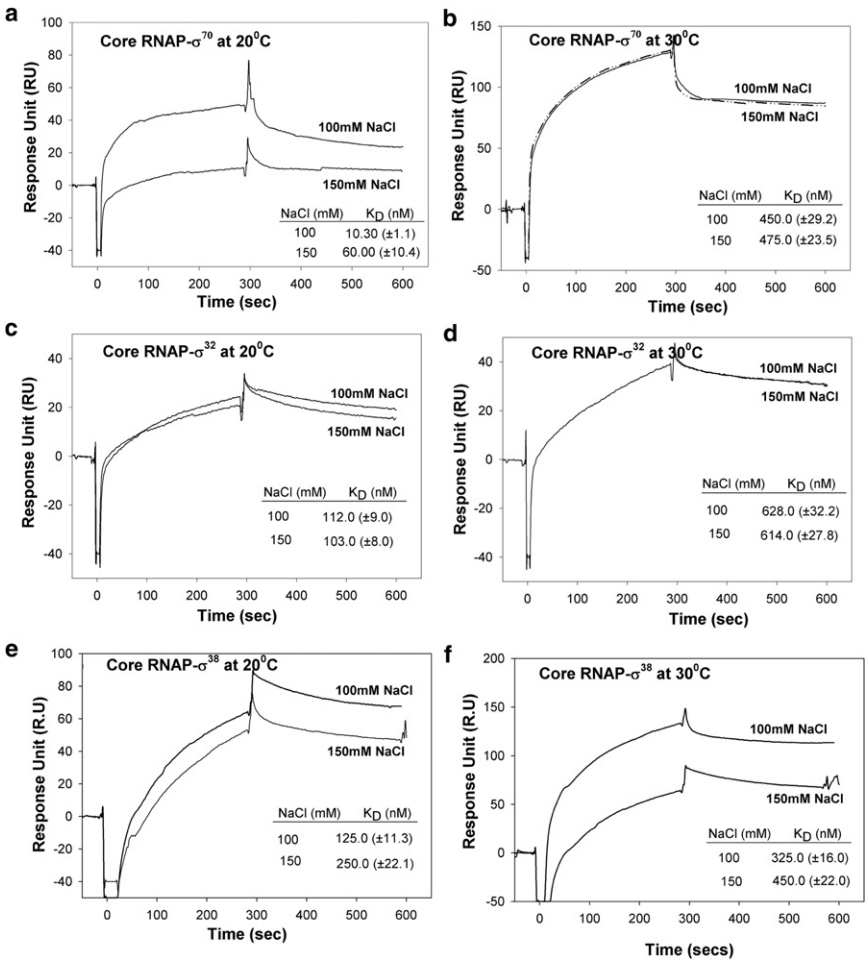

FIGURE 4 Comparative sensorgrams at different ionic strengths of 100 mM and 150 mM NaCl for the interaction of (*a*) core RNAP-σ^{70} at 20°C, (*b*) core RNAP-σ^{70} at 30°C, (*c*) core RNAP-σ^{32} at 20°C, (*d*) core RNAP-σ^{32} at 30°C, (*e*) core RNAP-σ^{38} at 20°C, and (*f*) core RNAP-σ^{38} at 30°C.

the presence of 100 mM and 150 mM NaCl at temperatures of 20°C and 30°C, respectively. In this case, the sensitivity to ionic strength was negligible at both temperatures. The salt sensitivity of σ^{38} binding to core RNAP is shown in Fig. 4, *e* and *f*. We observed a small amount of variation with changes in the osmolarity of the medium, but changes in temperature did not seem to affect this variation. This indicated that the salt sensitivity of the σ-factors varies as σ-32 < σ-38 < σ-70.

DISCUSSION

A comparison of the core binding affinity among the housekeeping σ-factor versus stress-related alternative σ-factors showed that the principal σ-factor (σ^{70}) has the strongest binding, with all other-factors remaining the same, and the weakest interaction was observed in the case of core RNAP binding to σ^{38} (σ^{s}). We observed a 12-fold difference in the core binding affinity of σ^{70} and σ^{38}, whereas that between the σ^{70} and σ^{32} core binding affinities was ~9-fold (Table 1). Our data indicate that core RNAP-σ binding, especially that obtained with σ^{70}, is extremely sensitive to changes in external stimuli. As such, it would be incorrect to predict an absolute order of binding affinities for these different σ-factors without taking into consideration the experimental variables. Thus, the order of relative binding affinity of the three σ-factors for the same core RNAP may be summarized as follows:

1. σ-32 < σ-38 < σ-70 (at 20°C, 150 mM NaCl).
2. σ-70 < σ-38 < σ-32 (at 20°C, 100 mM NaCl).
3. σ-32 < σ-38 < σ-70 (30–35°C, irrespective of salt concentration).
4. σ-70 < σ-32 < σ-38 (40°C).

It was previously noted that σ^{70} has a tendency to aggregate at higher concentrations (27), which may affect the interpretation of our kinetic data due to incorrect estimation of the monomeric form of σ-factor available to bind with core RNAP. Dynamic light scattering (DLS) and size exclusion chromatography studies were done to check the oligomeric status of the σ-factors. The DLS studies showed that at a concentration of 2 μM, all of the σ-factors had a polydispersity of <12%, indicating that they exist as a single homogeneous species (Fig. S6). The hydrodynamic radius calculated (R = 7.5 nm) for σ^{70} matched closely with that of the V-shaped crystal structure for σ^{70} (28). This indicates

that at this concentration, the purified σ-factors exist as a monomeric species. Beyond concentrations of 6 μM, the polydispersity increased to >16%, indicating that the population distribution was heterogeneous in nature and possibly consisted of a mixture of higher-order aggregates (Fig. S7). The fast protein liquid chromatography profile of the σ-factors also showed a single elution profile (Fig. S8), indicating a near absence of aggregates. In both the Langmuir trough and SPR studies, the proteins undergo a 100-fold dilution (nanomolar range), and as such would primarily consist of a homogeneous population of monomeric σ-factors (11) needed to bind to core RNAP. Hence, the differences in binding affinities observed were not related to σ-aggregation. The activity of the purified σ^{70} was checked in both multiple- and single-round in vitro promoter-specific transcription assays on a T7A1 promoter template (Fig. S8). A precise estimation of the functional amount of each σ was not possible here. However, we estimated the kinetic and thermodynamic parameters using saturation binding kinetics by varying the concentration range of σ within the molar ratio of 1:3 (core/σ). Thus, we ruled out the possibility that the rate of recruitment of σ-factors to core RNAP is dependent on the fraction of functional σ-factor present in each addition. The equilibrium binding studies reflect only the intrinsic binding affinities of σ-factors for core RNAP under varying physiological conditions and under conditions of molecular crowding (using a quasi-three-dimensional model, the surface density of immobilized molecules at the LB monolayer is estimated at 170–180 mg/ml) (16,25).

A molecular thermodynamic perspective of the core RNAP-σ interaction

Protein-protein interactions involving a single adduct formation from two individual partners are usually accompanied by an increase in the configurational entropy of the system. Thus, it is unique to have a negative entropy of interaction in the case of core RNAP binding to its σ-factors. This can only be explained if the interaction is accompanied by large-scale conformational changes of either interacting partner. A careful look at the σ^{70} domain organization indicates that the comparatively small 70 kDa protein must undergo distortions so that the conserved regions 2.1 and 2.3 can simultaneously make multiple contacts with both the β (150 kDa) and β' (155 kDa) subunits of RNAP (29,30). The energy for these conformational changes must be borrowed from the energy released during the electrostatic interactions between the charged protein lobes. Thus, the observed overall enthalpy for the core RNAP-σ interaction will be the excess energy released after allowing for conformational changes on the σ-factor. The smaller the released enthalpy, the greater will be the distortion involved for the σ-factor to make molecular contact with core RNAP and the magnitude of negative entropy. Therefore, the magnitude of the enthalpy and entropy values share an inverse relationship and can be used as a putative indicator for predicting the relative binding affinities of the three σ-factors. Evolutionary studies have shown that although they belong to the σ^{70} family of σ-factors, the alternative σ-factors (σ^{32} and σ^{38}) show a divergence in amino acid sequence from the conserved sequence of the principal σ-factor (σ^{70}) (31,32). This relaxation in conserved amino acid sequences may be compensated for by a more stringent demand for binding domain recognition to enable an interaction to take place. Thus, the alternative σ-factors would have to undergo greater structural distortion to interact with core RNAP as compared with $-\sigma^{70}$. This would account for the observed lower free energy of interaction and smaller amount of enthalpy released for core RNAP interacting with σ^{32}/σ^{38} at 25°C as compared with the same for core RNAP binding to σ^{70} at this temperature (33,34). Thus, thermal energy and osmolarity could act as regulators in preventing a nonoptimized binding of σ-factors depending on the changing physiological conditions. This hypothesis accords well with our observed changes in binding affinity (Tables 1 and 2) and puts our understanding of the structural and molecular implications of domain organization in σ-factors on a solid basis (35,36).

Comparison of the LB technique and SPR

It is evident from the data presented here that the sensitivity of the detection method used plays a significant role in determining the value of the binding parameters. Unlike the thermodynamic parameters of a system, which are its intrinsic variables and define the system at equilibrium (Table S2), the kinetic binding parameters are extrinsic variables and depend on the imposed conditions. As such, we observe a 10- to 100-fold variation in the kinetic parameters obtained using two different nonhomogeneous methods (Table 3). Although both the SPR and LB techniques function on the principle of partitioning of reactants between the bulk phase and the interface, their detection methods have intrinsic differences that are reflected in the respective quantitative evaluations. In the case of the LB monolayer, one can circumvent the problem of mass transport by evaluating the binding parameters only after the system has reached equilibrium (22,25). However, for SPR, where interactions are followed in real time, mass transport will affect the observed rate constant. The heterogeneity of covalent linkage formation in SPR may also compromise the availability of the σ-interaction domains, whereas site-directed immobilization at the LB monolayer ensures that the core RNAP-σ binding interfaces remain unaffected (37). In terms of data analysis and interpretation, the saturation binding analysis used in the LB technique allows for inhomogeneous data points to be evenly spaced out along a linear fit and gives a better idea of the binding. However, the use of

TABLE 3 (a) Comparison of macroscopic equilibrium dissociation constant values for core RNAP-σ^{70} interaction

Temperature	Evaluation of K_D (M) by SPR	Evaluation of K_D (M) by LB
20°C	$6.00\ (\pm 1.04) \times 10^{-8}$	$1.25\ (\pm 0.22) \times 10^{-9}$
25°C	$2.01\ (\pm 0.23) \times 10^{-7}$	$5.00\ (\pm 0.66) \times 10^{-9}$
30°C	$4.75\ (\pm 0.23) \times 10^{-7}$	$9.09\ (\pm 0.71) \times 10^{-9}$
40°C	$3.00\ (\pm 1.7) \times 10^{-6}$	$1.58\ (\pm 0.17) \times 10^{-8}$

TABLE 3 (b) Comparison of macroscopic equilibrium dissociation constant values for core RNAP-σ^{32} interaction

Temperature	Evaluation of K_D (M) by SPR	Evaluation of K_D (M) by LB
20°C	$1.03\ (\pm 0.08) \times 10^{-7}$	$2.25\ (\pm 0.11) \times 10^{-8}$
25°C	$3.12\ (\pm 0.21) \times 10^{-7}$	$5.71\ (\pm 0.28) \times 10^{-8}$
30°C	$6.14\ (\pm 0.27) \times 10^{-7}$	$7.29\ (\pm 0.34) \times 10^{-8}$
40°C	$1.72\ (\pm 0.14) \times 10^{-6}$	$1.25\ (\pm 0.08) \times 10^{-7}$

TABLE 3 (c) Comparison of macroscopic equilibrium dissociation constant values for core RNAP-σ^{38} interaction

Temperature	Evaluation of K_D (M) by SPR	Evaluation of K_D (M) by LB
20°C	$2.50\ (\pm 0.22) \times 10^{-7}$	$5.90\ (\pm 0.39) \times 10^{-8}$
25°C	$3.25\ (\pm 0.23) \times 10^{-7}$	$6.12\ (\pm 0.49) \times 10^{-8}$
30°C	$4.50\ (\pm 0.22) \times 10^{-7}$	$6.25\ (0.\pm 56) \times 10^{-8}$

the Marquardt-Levenberg algorithm for curve-fitting in SPR (Table S3) ensures a smaller window of deviation for the values calculated. Similarly, when it comes to maintaining the osmolarity of the solution closer to physiological conditions, the SPR technique (100–150 mM NaCl) has an advantage over the LB method (10 mM NaCl).

Despite the differences in estimated kinetic parameters between the LB and SPR methods, the data sets generated for each technique were internally consistent. Further, although there was variability in absolute values, the relative order of σ-affinity for core RNAP under given experimental conditions was found to be consistent for both measurements. Thus, based on the analysis of data sets from individual techniques, as well as a comparison of data obtained under different experimental conditions, we may conclude that both salt and temperature play a major role in determining the degree of σ-switching.

CONCLUSIONS

By estimating the binding parameters for different σ-factors under the same experimental conditions, we were able to reach a consensus regarding the relative binding of σ-factors for the same core. The susceptibility of this interaction to external stimuli suggests that there is no absolute order for the relative binding affinities of σ-factors for core RNAP. Rather, it appears that bacteria themselves have adapted so that they can coordinate their gene expression profile based on environmental variables. The use of an equilibrium binding model to evaluate the kinetic variables reduced the possibility of inaccuracy in measurements associated with partitioning of components between two phases, and the reduced dimensionality of our system allowed us to study the interaction under conditions of macromolecular crowding (170–180 mg/ml). The system can also be used as a model system for exploring other biologically relevant protein-protein competitive interactions, which represent a promising class of therapeutic targets.

SUPPORTING MATERIAL

Data related to details of protein purification, reconstitution of core RNAP and generation of Scatchard plots and van 't Hoff plots used for the kinetic and thermodynamic analysis are available at http://www.biophysj.org/biophysj/supplemental/S0006-3495(12)00874-0.

We thank Ms. Sreelatha for the SPR studies, AstraZeneca for the σ^{70} strain, and Prof. Akira Ishihama (Hosei University, Tokyo, Japan) for the σ^{32} and σ^{38} strains.

D.C. received support from the Department of Science and Technology, India, and A.G. received a Senior Research Fellowship from the Council for Scientific and Industrial Research.

REFERENCES

1. deHaseth, P. L., M. L. Zupancic, and M. T. Record, Jr. 1998. RNA polymerase-promoter interactions: the comings and goings of RNA polymerase. *J. Bacteriol.* 180:3019–3025.
2. Helmann, J. D., and M. J. Chamberlin. 1988. Structure and function of bacterial σ-factors. *Annu. Rev. Biochem.* 57:839–872.
3. Lonetto, M., M. Gribskov, and C. A. Gross. 1992. The σ70 family: sequence conservation and evolutionary relationships. *J. Bacteriol.* 174:3843–3849.
4. Losick, R., and J. Pero. 1981. Cascades of σ-factors. *Cell.* 25:582–584.
5. Ishihama, A. 2000. Functional modulation of *Escherichia coli* RNA polymerase. *Annu. Rev. Microbiol.* 54:499–518.
6. Vicente, M., K. F. Chater, and V. De Lorenzo. 1999. Bacterial transcription-factors involved in global regulation. *Mol. Microbiol.* 33:8–17.
7. Grigorova, I. L., N. J. Phleger, …, C. A. Gross. 2006. Insights into transcriptional regulation and σ competition from an equilibrium model of RNA polymerase binding to DNA. *Proc. Natl. Acad. Sci. USA.* 103:5332–5337.
8. Wu, F. Y., L. R. Yarbrough, and C. W. Wu. 1976. Conformational transition of *Escherichia coli* RNA polymerase induced by the interaction of σ subunit with core enzyme. *Biochemistry.* 15:3254–3258.
9. Glaser, T. B., V. Bergendahl, …, R. R. Burgess. 2009. Studying the salt dependence of the binding of σ70 and σ32 to core RNA polymerase using luminescence resonance energy transfer. *PLoS ONE.* 4:1–11.
10. Maeda, H., N. Fujita, and A. Ishihama. 2000. Competition among seven *Escherichia coli* σ subunits: relative binding affinities to the core RNA polymerase. *Nucleic Acids Res.* 28:3497–3503.
11. Ferguson, A. L., A. D. Hughes, …, J. G. Hoggett. 2000. Interaction of σ^{70} with *Escherichia coli* RNA polymerase core enzyme studied by surface plasmon resonance. *FEBS Lett.* 481:281–284.
12. Völker, J., and K. J. Breslauer. 2005. Communication between noncontacting macromolecules. *Annu. Rev. Biophys. Biomol. Struct.* 34:21–42.
13. Burgess, R. R., A. A. Travers, …, E. K. Bautz. 1969. -factor stimulating transcription by RNA polymerase. *Nature.* 221:43–46.
14. Tanaka, K., Y. Takayanagi, …, H. Takahashi. 1993. Heterogeneity of the principal σ-factor in *Escherichia coli*: the rpoS gene product,

σ38, is a second principal σ-factor of RNA polymerase in stationary-phase *Escherichia coli*. *Proc. Natl. Acad Sci. USA*. 90:3511–3515.

15. Zhao, K., M. Liu, and R. R. Burgess. 2005. The global transcriptional response of *Escherichia coli* to induced σ32 protein involves σ32 regulon activation followed by inactivation and degradation of σ32 in vivo. *J. Biol. Chem.* 280:17758–17768.
16. Ganguly, A., and D. Chatterji. 2011. Sequential assembly of an active RNA polymerase molecule at the air-water interface. *Langmuir.* 27:3808–3814.
17. Ghosh, P., A. Ishihama, and D. Chatterji. 2001. *Escherichia coli* RNA polymerase subunit omega and its N-terminal domain bind full-length β' to facilitate incorporation into the $\alpha 2\beta$ subassembly. *Eur. J. Biochem.* 268:4621–4627.
18. Tang, H., K. Severinov, …, R. H. Ebright. 1995. Rapid RNA polymerase genetics: one-day, no-column preparation of reconstituted recombinant *Escherichia coli* RNA polymerase. *Proc. Natl. Acad. Sci. USA*. 92:4902–4906.
19. Brar, L. K., P. Rajdev, …, D. Chatterji. 2005. Langmuir monolayer as a tool toward visualization of a specific DNA-protein complex. *Langmuir.* 21:10671–10675.
20. Gaines, G. L. 1966. Insoluble Monolayers at Liquid-Gas Interfaces. Wiley-Interscience, New York.
21. Robert, G. 1990. Langmuir-Blodgett Films. Plenum Press, New York/London.
22. Yang, L., M. E. Biswas, and P. Chen. 2003. Study of binding between protein A and immunoglobulin G using a surface tension probe. *Biophys. J.* 84:509–522.
23. Rajdev, P., and D. Chatterji. 2007. Thermodynamic and spectroscopic studies on the nickel arachidate-RNA polymerase Langmuir-Blodgett monolayer. *Langmuir.* 23:2037–2041.
24. Leirmo, S., C. Harrison, …, M. T. Record, Jr. 1987. Replacement of potassium chloride by potassium glutamate dramatically enhances protein-DNA interactions *in vitro*. *Biochemistry.* 26:2095–2101.
25. Ganguly, A., P. Rajdev, and D. Chatterji. 2009. Sequence specific interaction between promoter DNA and *Escherichia coli* RNA polymerase: comparative thermodynamic analysis with one immobilized partner. *J. Phys. Chem. B.* 113:15399–15408.
26. Nonaka, G., M. Blankschien, …, V. A. Rhodius. 2006. Regulon and promoter analysis of the *E. coli* heat-shock-factor, σ32, reveals a multifaceted cellular response to heat stress. *Genes Dev.* 20:1776–1789.
27. Zhi, H., and D. J. Jin. 2003. Purification of highly-active and soluble *Escherichia coli* σ^{70} polypeptide overproduced at low temperature. *Methods Enzymol.* 370:174–180.
28. Malhotra, A., E. Severinova, and S. A. Darst. 1996. Crystal structure of a σ^{70} subunit fragment from *E. coli* RNA polymerase. *Cell.* 87:127–136.
29. Arthur, T. M., L. C. Anthony, and R. R. Burgess. 2000. Mutational analysis of β'260-309, a σ70 binding site located on *Escherichia coli* core RNA polymerase. *J. Biol. Chem.* 275:23113–23119.
30. Callaci, S., E. Heyduk, and T. Heyduk. 1998. Conformational changes of *Escherichia coli* RNA polymerase σ70 -factor induced by binding to the core enzyme. *J. Biol. Chem.* 273:32995–33001.
31. Gruber, T. M., and C. A. Gross. 2003. Multiple σ subunits and the partitioning of bacterial transcription space. *Annu. Rev. Microbiol.* 57:441–466.
32. Sharp, M. M., C. L. Chan, …, C. A. Gross. 1999. The interface of σ with core RNA polymerase is extensive, conserved, and functionally specialized. *Genes Dev.* 13:3015–3026.
33. Zhou, Y. N., W. A. Walter, and C. A. Gross. 1992. A mutant σ32 with a small deletion in conserved region 3 of σ has reduced affinity for core RNA polymerase. *J. Bacteriol.* 174:5005–5012.
34. Gopal, V., H. W. Ma, …, D. Chatterji. 1994. A point mutation at the junction of domain 2.3/2.4 of transcription -factor σ70 abrogates productive transcription and restores its expected mobility on a denaturing gel. *J. Mol. Biol.* 242:9–22.
35. Chan, C. L., M. A. Lonetto, and C. A. Gross. 1996. σ Domain structure: one down, one to go. *Structure.* 4:1235–1238.
36. Gruber, T. M., D. Markov, …, C. A. Gross. 2001. Binding of the initiation -factor σ(70) to core RNA polymerase is a multistep process. *Mol. Cell.* 8:21–31.
37. Zimmermann, J. L., T. Nicolaus, …, K. Blank. 2010. Thiol-based, site-specific and covalent immobilization of biomolecules for single-molecule experiments. *Nat. Protoc.* 5:975–985.